Pertanika J. Sci. & Technol. 31 (6): 3107 - 3124 (2023)

SCIENCE & TECHNOLOGY

Journal homepage: http://www.pertanika.upm.edu.my/

Adaptive Threshold-based Fault Detection for Systems Exposed to Model Uncertainty and Deterministic Disturbance

Masood Ahmad[1,2] and Rosmiwati Mohd-Mokhtar[1]*

[1]School of Electrical and Electronic Engineering, Universiti Sains Malaysia, Engineering Campus, 14300 Nibong Tebal, Pulau Pinang, Malaysia
[2]Department of Electrical and Computer Engineering, COMSATS University Islamabad (Lahore Campus) Lahore, Pakistan

ABSTRACT

The fault detection problem is investigated for discrete-time linear uncertain systems. Instead of designing a fault detection system from the viewpoint of observer design for robust residual generation, an adaptive threshold approach is proposed to attain robustness against disturbance and norm-bounded model uncertainty. The main goal of the research is to develop a threshold design method that could establish an appropriate trade-off between false alarms and missed fault detection in the presence of model uncertainty. For this purpose, the H_∞ optimization technique is adopted in the linear matrix inequality framework to compute the unknown parameters of an adaptive threshold. It is shown that the proposed fault detection system based on an adaptive threshold depends only on the system parameters and the control input of the monitored system. It is independent of robust residual generator designs in traditional observer-based fault detection systems. The effectiveness of the proposed approach is verified on two well-known benchmark systems: a direct-current motor and three tank systems. Several types of faults are successfully detected in both applications.

Keywords: Adaptive threshold, fault detection, H_∞ optimization, linear matrix inequality, model uncertainty

ARTICLE INFO

Article history:
Received: 27 November 2022
Accepted: 04 April 2023
Published: 09 October 2023

DOI: https://doi.org/10.47836/pjst.31.6.26

E-mail addresses:
masoodjaffar@student.usm.my (Masood Ahmad)
eerosmiwati@usm.my (Rosmiwati Mohd-Mokhtar)
* Corresponding author

INTRODUCTION

The reliability and safety of engineering systems remain the prime focus as technology advances. In this regard, several sophisticated systems have been developed with the aid of advanced and robust control theories that ensure the desired performance

ISSN: 0128-7680
e-ISSN: 2231-8526

of the system. The performance is governed by the system's internal components and by the functionality of sensors and actuators (Ahmad & Mohd-Mokhtar, 2021; Rahnavard et al., 2019).

Faults in these critical parts significantly reduce the system's overall performance and, in some cases, put the system in danger if not handled immediately. Fault detection (FD) plays a vital role in such situations by promptly identifying the presence of a fault and assisting in preventing both financial and fatal losses (Na & Ahmad, 2019; Salimi et al., 2019).

In the existing literature, FD techniques are typically classified as data-driven and model-based (Chen & Patton, 2012; Ding, 2014). The data-driven approach is adopted when system dynamics cannot be quantitatively modeled due to insufficient knowledge of the system's internal behavior. In contrast to data-driven techniques, model-based FD is chosen based on knowledge of the system dynamics, and mathematical model equations are developed. These equations are used to reconstruct the system output and verify that the anticipated output is consistent with the measured output from the sensors. The output error is treated as a residual. It should ideally be zero if there is no fault and non-zero otherwise.

Model-based FD techniques are further categorized as parameter estimation techniques, observer-based techniques, and parity relation techniques. In this study, the focus is on the observer-based technique. This technique consists of residual generation and evaluation, including threshold design. The primary task of the first stage, i.e., residual generation, is to generate a residual that indicates the possible occurrence of the fault. In the second stage, the residual is evaluated using signal and system norms to distinguish the fault from disturbance and noise and then compared with the threshold (Ahmad & Mohd Mokhtar, 2022; Gertler, 2017). Finally, a fault is declared upon simple decision logic, in which if the evaluated residual exceeds the threshold, the fault is declared and vice versa.

Most practical systems encounter unknown inputs, i.e., deterministic disturbance and/or random noise and model uncertainties. The unknown inputs cause deviation in the residual from zero in fault-free cases, which ultimately reduces the FD system performance. Thus, an indispensable need is to design a robust FD system where these unknown inputs are treated very carefully. In this context, two approaches have been used to deal with these unknown inputs in a model-based framework. In the first method, the residual generator is designed to either generate a residual completely decoupled from unknown inputs or use optimization approaches to make the residual robust against unknown inputs. Robust residual generation using optimization approaches has gained much attention, and very good results have been reported for linear systems subjected to unknown disturbance and random noise in the existing literature (Blanke et al., 2015; Gertler, 2017; Isermann, 2006). It is worth mentioning that generated residuals satisfy the sensitivity and robustness criterion in terms of performance indexes such as H_∞/H_∞, H_-/H_∞, and H_2/H_∞. In the second approach, rather than designing a robust residual generator, a robust threshold is designed to handle the unknown inputs in the residual evaluation stage.

More specifically, in the former case, an observer is designed to produce an unbiased estimation of the system's outputs, irrespective of the influence of model uncertainties and unknown disturbances that make output error zero, a desired phenomenon in FD. Robust residual generation is only possible when the observer design meets the robustness and sensitivity requirements of certain performance indexes. In the latter case, robustness to model uncertainties and unknown disturbances is ensured by a robust threshold in the residual evaluation stage rather than the residual generation stage (Amirkhani et al., 2020; Raka & Combastel, 2013; Puig et al., 2013; Montes de Oca et al., 2012). A robust threshold determines the maximum tolerance limit of an unknown disturbance and model uncertainty of the residual in the fault-free case. This approach eliminates the need for a separate robust residual generator design. The separate design of robust residual generation refers to an independent design of an observer, which is not linked with the threshold design in the second stage. In this case, the observer and threshold are designed separately for successful FD (former case). In robust threshold design, the threshold is designed in such a way that it could minimize the effect of the unknown inputs. Residual generation and threshold design are integrated into a single stage.

On the other side, the main challenges in the robust threshold design are false alarms and missed detection of the faults that must be addressed for successful FD. False alarms are generated due to unknown inputs, which forces the residual to cross the threshold even in fault-free cases. In this study, a threshold is designed for linear discrete-time systems subjected to norm-bounded model uncertainty and deterministic disturbances, which is the main contribution and becomes the paper's objective that distinguishes it from the existing literature. In this paper, the residual is generated by a fault detection filter (FDF), and the H_∞ optimization technique is used in the linear matrix inequality (LMI) framework to calculate the unknown parameters of the threshold. In the proposed threshold design, the maximum influence of unknown disturbance and model uncertainty is not considered, compared to the standard threshold, which reduces the missed detection of the fault because of the lower value of the detection threshold and increases the false alarms in the system. In the end, a DC motor and three-tank system illustrate the significance of the proposed scheme via simulations. The effectiveness of the proposed threshold in detecting the fault is assessed using a variety of sensor and actuator faults.

PROBLEM FORMULATION

A linear discrete-time dynamic system, driven by l_2 norm bounded control input $u(k) \in R^p$, unknown input $d(k) \in R^{k_d}$, and affected by $f(k) \in R^{k_f}$ and model uncertainties (Δs) is represented by the following Equation 1:

$$x(k+1) = (A + \Delta A)x(k) + (B + \Delta B)u(k) + E_d d(k) + E_f f(k)$$
$$y(k) = (C + \Delta C)x(k) + (D + \Delta D)u(k) + F_d d(k) + F_f f(k) \quad (1)$$

where $x(k) \in R^n$ denotes the state vector and $y(k) \in R^m$ be the measurement vector. $A, B, C, D, E_d, F_d, E_f$, and F_f are known matrices with appropriate dimensions. $\Delta A, \Delta B, \Delta C, \Delta D$ are norm-bounded model uncertainties, defined as Equation 2:

$$\begin{bmatrix} \Delta A & \Delta B \\ \Delta C & \Delta D \end{bmatrix} = \begin{bmatrix} H_1 \sum G_1 & H_1 \sum G_2 \\ H_2 \sum G_1 & H_2 \sum G_2 \end{bmatrix} \quad (2)$$

where H_1, H_2, G_1 and G_2 are known matrices with compatible dimensions, and Σ is an unknown scalar constant but bounded with a condition that holds $\sum^T \sum \leq \delta$ and $0 < \delta \leq 1$. Furthermore, it is assumed that $\sup_{d \neq 0} \|d(k)\|_2 \leq \delta_d$, where δ_d is the upper limit of energy of unknown disturbance. Note that δ_d and δ represent the maximum possible influence of disturbance and model uncertainty on the system dynamics.

Observer-based residual generator, so-called FDF, is described by Equation 3:

$$\hat{x}(k+1) = A\hat{x}(k) + Bu(k) +$$
$$r(k) = y(k) - \hat{y}(k) \quad (3)$$
$$\text{where } \hat{y}(k) = C\hat{x}(k) + Du(k)$$

$\hat{x}(k)$ is a state estimation vector, $\hat{y}(k) \in R^m$ is the estimated output vector, and $r(k)$ is the residual signal. The new vector, i.e., state estimation error vector, $e(k) = x(k) - \hat{x}(k)$, illustrates the dynamics of FDF (Equation 3) and is described by Equations 4 and 5:

$$e(k+1) = (A - LC)e(k) + (\Delta A - L\Delta C)x(k) + (\Delta B - L\Delta D)u(k) +$$
$$(E_d - LF_d)d(k) + \left(E_f - LF_f\right) f(k) \quad (4)$$

$$Ce(k) + \Delta Cx(k) + \Delta Du(k) + F_d d(k) + F_f f(k) \quad (5)$$

It is evident from Equation 5 that residual is sensitive to fault as well as unknown input, control input, and system's state. For residual evaluation purposes, the l_2 norm of the residual Equation 5 is used and can be expressed as Equation 6:

$$J(k) = \|r(k)\|^2_{2,[k,k+N]} = \sum_{j=0}^{N} r^T(k+j)r(k+j) \quad (6)$$

Recall that the l_2 norm of a signal evaluates the change in energy of a signal in a certain evaluation window ($k,k+N$). For FD purposes, it is desired to use the energy of the residual signal as an evaluation function rather than the residual's maximum/minimum peak value.

Furthermore, the standard threshold for FD is defined as Equation 7:

$$J_{th} = \sup_{\sum^T \sum \leq \delta I, \|d(k)\|_2 \leq \delta_d, f=0} \|r(k)\|_2^2 \tag{7}$$

It is evident from Equation 7 that the threshold represents the maximum value of the residual energy under the maximum possible influence of disturbance and model uncertainty in fault-free cases, leading the false alarms to zero. On the other hand, residual signals with small faults cannot cross the threshold because the fault signal disappears in the residual, ultimately increasing the missed detection of the faults.

New variables are defined below for designing a proposed threshold.

$\delta_{dd} \leq \delta_d$ and $\delta_{\Delta s} \leq \delta$

where δ_{dd} and $\delta_{\Delta s}$ represent the influence of certain energy levels of disturbance and model uncertainty on the system, respectively. The following threshold is proposed (Equation 8) to decrease the missed detection of the faults:

$$J_{th} = \sup_{\sum^T \sum \leq \delta_{\Delta s} I, \|d(k)\|_2 \leq \delta_{dd}, f=0} \|r(k)\|_2^2 \tag{8}$$

The threshold in Equation 8 determines the maximum change in energy of the $r(k)$ when $r(k)$ is influenced by disturbance and model uncertainty of a certain energy level, i.e.,δ_{dd} and $\delta_{\Delta s}$, rather than the maximum possible influence, i.e., δ_d and δ. Setting the threshold according to Equation 8 decreases the missed detection of the faults. On the other hand, disturbance $\|d(k)\|_2 > \delta_{dd}$ and model uncertainty $\Delta A, \Delta B, \Delta C, \Delta D$ in which $\sum^T \sum > \delta_{\Delta s} I$ force the residual $r(k)$ to cross the J_{th} in Equation 8 in fault-free cases lead to an increase in false alarms. Thus, there is a need to develop a method of threshold design for FD in the uncertain system in Equation 1 that can establish a suitable trade-off between missed detection of faults and false alarms. Following Equation 8, the proposed threshold in a fault-free case can be written as Equations 9 and 10:

$$J_{th} = \sup_{\sum^T \sum \leq \delta_{\Delta s} I, \|d(k)\|_2 \leq \delta_{dd}, f=0} \|G_{ru}(z)u(z) + G_{rd}(z)d(z)\|_2 \tag{9}$$

$$J_{th} = \sup_{\sum^T \sum \leq \delta_{\Delta s} I, \|d(k)\|_2 \leq \delta_{dd}, f=0} (\|G_{ru}(z)u(z)\|_2 + \|G_{rd}(z)d(z)\|_2) \tag{10}$$

where G_{ru} and G_{rd} represent the transfer function matrices from u and d to r

$$G_{ru} = C(zI - A + LC)^{-1}(\varDelta B - L\varDelta D) + \varDelta$$

$$G_{rd} = C(zI - A + LC)^{-1}(E_d - LF_d) + F_d$$

Lemma 1: Let $B: S_1 \rightarrow S_2$ are two systems with appropriate dimensions and $S_1, S_2 \in (0, \infty]$ then $\|AB\|_2 \leq \|A\|_\infty \|B\|_2$

Applying Lemma 1 on Equation 10 leads to Equations 11, 12, and 13:

$$J_{th} = \sup_{\Sigma^T \Sigma \leq \delta_{\Delta s} I, \|d(k)\|_2 \leq \delta_{dd}, f = 0} (\|G_{ru}(z)\|_\infty \|u(z)\|_2 + \|G_{rd}(z)\|_\infty \|d(z)\|_2) \quad (11)$$

$$J_{th} = \sup_{\Sigma^T \Sigma \leq \delta_{\Delta s} I, \|d(k)\|_2 \leq \delta_{dd}, f = 0} (\gamma_u \|u(z)\|_2 + \gamma_d \|d(z)\|_2) \quad (12)$$

$$J_{th} = \sup_{\Sigma^T \Sigma \leq \delta_{\Delta s} I, \|d(k)\|_2 \leq \delta_{dd}, f = 0} (\gamma_u \|u(z)\|_2 + \gamma_d \delta_{dd}) \quad (13)$$

δ_{dd} is the certain energy level of unknown disturbance, which is assumed to be known. $\|u\|_2$ is the l_2 norm of the control input, generally known in practical systems. The control input varies during the system operation, eventually changing the FD threshold. Such a threshold is an adaptive threshold, which depends on the real values of system input. Thus, the aim here is to find the unknown parameters of the threshold in Equation 8, i.e., γ_u and γ_d.

METHOD TO FIND THE UNKNOWN PARAMETERS

A frequency domain representation of the residual in Equation 5 is written as Equation 14:

$$r(z) = G_{rd}(z)d(z) + G_{rf}(z)f(z) + G_{r\bar{u}}(z)\bar{u}(z) \quad (14)$$

where $G_{r\bar{u}}, G_{rd}$, and G_{rf} represent the transfer function matrices from $\bar{u}, d$, and f to r

$$G_{r\bar{u}} = \left[C(zI - A + LC)^{-1}[(\Delta A - L\Delta C) \quad (\Delta B - L\Delta D)] + [\Delta C \quad \Delta D]\right]$$
$$G_{rd} = C(zI - A + LC)^{-1}(E_d - LF_d) + F_d$$
$$G_{rf} = C(zI - A + LC)^{-1}\left(E_f - LF_f\right) + F_f$$

and $\bar{u}(z) = \begin{bmatrix} x(z) \\ u(z) \end{bmatrix}$

In Equation 14, $G_{r\bar{u}}(z)\bar{u}(z)$ contains uncertain system matrices. Therefore, it is separately treated as written in Equations 15 and 16:

$$[\Delta A - L\Delta C \quad \Delta B - L\Delta D] \begin{bmatrix} x(z) \\ u(z) \end{bmatrix} + [\Delta C \quad \Delta D] \begin{bmatrix} x(z) \\ u(z) \end{bmatrix} \quad (15)$$

$$(H_1 - LH_2)\Sigma[G_1 \quad G_2] \begin{bmatrix} x(z) \\ u(z) \end{bmatrix} + H_2 \Sigma[G_1 \quad G_2] \begin{bmatrix} x(z) \\ u(z) \end{bmatrix} \quad (16)$$

From Equation 16, defining a new variable as in Equation 17:

$$B_a = [G_1 \quad G_2]\begin{bmatrix} x(z) \\ u(z) \end{bmatrix} = G_1 x(z) + G_2 u(z) \tag{17}$$

where $x(z) = (zI - A - \Delta A)^{-1}[B + \Delta B \quad E_d]\begin{bmatrix} u(z) \\ d(z) \end{bmatrix}$. $x(z)$ is the dynamic response of B_a subject to unknown disturbance d and known control input u. Hence, Equation 17 becomes Equation 18:

$$B_a = G_1(zI - A - \Delta A)^{-1}(B + \Delta B \quad E_d) + (G_2 \quad 0)\begin{bmatrix} u(z) \\ d(z) \end{bmatrix} \tag{18}$$

By using Equation 18, Equation 16 can be written as Equation 19:

$$(H_1 - LH_2)\sum B_a + H_2 \sum B_a \tag{19}$$

By incorporating Equation 19 into Equation 14, it can be expanded to Equations 20, 21, 22, and 23:

$$r(z) = [C(zI - A + LC)^{-1}(E_d - LF_d) + F_d]\, d(z) + \left[C(zI - A + LC)^{-1}\left(E_f - LF_f\right) + F_f\right] f(z) + C(zI - A + LC)^{-1}[(H_1 - LH_2) + H_2]\sum B_a \tag{20}$$

$$r(z) = [C(zI - A + LC)^{-1}(H_1 - LH_2 \quad E_d - LF_d) + (H_2 \quad F_d)]\begin{bmatrix} \sum B_a \\ d(z) \end{bmatrix} + \left[C(zI - A + LC)^{-1}\left(E_f - LF_f\right) + F_f\right] f(z) \tag{21}$$

$$r(z) = [C(zI - A + LC)^{-1}(H_1 \quad E_d) - L(H_2 \quad F_d) + (H_2 \quad F_d)]\begin{bmatrix} \sum B_a \\ d(z) \end{bmatrix} + + \left[C(zI - A + LC)^{-1}\left(E_f - LF_f\right) + F_f\right] f(z) \tag{22}$$

$$r(z) = [C(zI - A + LC)^{-1}(\bar{E}_{\bar{\bar{u}}} - L\bar{F}_{\bar{\bar{u}}}) + \bar{F}_{\bar{\bar{u}}}]\bar{\bar{u}}(z) + [C(zI - A + LC)^{-1}\left(E_f - LF_f\right) + F_f] f(z) \tag{23}$$

where

$$\bar{\bar{u}}(z) = \begin{bmatrix} \sum B_a \\ d(z) \end{bmatrix},\ \bar{E}_{\bar{\bar{u}}} = (H_1 \quad E_d) \text{ and } \bar{F}_{\bar{\bar{u}}} = (H_2 \quad F_d)$$

Finally, the expression for the residual signal is written as Equation 24:

$$r(z) = G_{r\overline{ud}}(z)\bar{\bar{u}}(z) + G_{rf}(z) f(z) \tag{24}$$

By using the residual signal in Equation 24, the proposed threshold in Equation 8 in a fault-free case can be expressed as Equation 25:

$$J_{th} = \sup_{\sum^T \sum \leq \delta_{\Delta s} I,\ \|d(k)\|_2 \leq \delta_{dd},\ f = 0} \|G_{r\overline{ud}}(z)\bar{\bar{u}}(z)\|_2 \tag{25}$$

Applying Lemma 1, Equation 25 turns to Equations 26, 27 and 28:

$$J_{th} = \|G_{r\overline{ud}}(z)\|_\infty \sup_{\sum^T\sum \le \delta_{\Delta s}I, \|d(k)\|_2 \le \delta_{dd}, f=0} \|\bar{\bar{u}}(z)\|_2 \tag{26}$$

$$J_{th} = \|G_{r\overline{ud}}\|_\infty \sup_{\sum^T\sum \le \delta_{\Delta s}I, \|d(k)\|_2 \le \delta_{dd}, f=0} \left\|\begin{matrix}\sum B_a \\ d(z)\end{matrix}\right\|_2 \tag{27}$$

$$J_{th} = \|G_{r\overline{ud}}\|_\infty \sup_{\sum^T\sum \le \delta_{\Delta s}I, \|d(k)\|_2 \le \delta_{dd}, f=0} \|\sum\|_2 . \|B_a\|_2 + +\|d(z)\|_2 \tag{28}$$

Assuming the bounds on $d, \sum$, i.e.,$\|d\|_2 \le \delta_{dd}, \sum^T\sum \le \delta_{\Delta s}I$, the threshold turns to Equation 29:

$$J_{th} = \|G_{r\overline{ud}}\|_\infty (\delta_{\Delta s})\|B_a\|_2 + \delta_{dd} \tag{29}$$

By carefully observing Equation 18, it is clear that B_a is the output of the system driven by the inputs u and d, and it can be described as Equation 30:

$$G_{B_a} = G_1(zI - A - \Delta A)^{-1}(B + \Delta B \quad E_d) + (G_2 \quad 0) \tag{30}$$

Using Lemma 1, it is reasonable to write Equation 31:

$$\|B_a\|_2 \le \left\|G_{B_a}\right\|_\infty . (\delta_{dd} + \|u\|_2) \tag{31}$$

Hence, Equation 29 turns to Equation 32:

$$J_{th} = \|G_{r\overline{ud}}\|_\infty (\delta_{\Delta s})[\left\|G_{B_a}\right\|_\infty (\delta_{dd} + \|u\|_2)] + \delta_{dd} \tag{32}$$

In Equation 32, all the parameters of the proposed threshold are known except the H-infinity norm of G_{B_a} and $G_{r\overline{ud}}$. Theorem 1 presents a method to determine the H-infinity norm of G_{B_a}. Due to space constraints, the proof is omitted here but can be obtained by solving a bounded real lemma (Boyd et al., 1994).

Theorem 1: For discrete-time linear uncertain system (Equation 33):

$$x(k+1) = \bar{\bar{A}}x(k) + \bar{\bar{B}}ud(k)$$

$$y(k) = \bar{\bar{C}}\, x(k) + \bar{\bar{D}}\, ud(k) \tag{33}$$

where $\bar{\bar{A}} = (A + \Delta A)$, $\bar{\bar{B}} = [B + \Delta B \quad E_d]$, $\bar{\bar{C}} = G_1$

$\bar{\bar{D}} = [G_2 \quad 0]$, $\Delta A = H_1\sum G_1$, $\Delta B = H_1\sum G_2$

$\bar{B} = [B \quad E_d]$, and $\sum^T\sum \le \delta I$

Given $\gamma > 0$, if there exists a scalar $\varepsilon > 0$ and positive definite matrix $P > 0$ such that the following LMI in Equation 34 holds, then the system in Equation 33 is asymptotically stable, and the H_∞ norm of transfer function G_{yud} satisfies $\|G_{yud}\|_\infty < \gamma$.

$$\begin{bmatrix} -\varepsilon I & 0 & 0 & {H_1}^T & 0 & 0 \\ * & -P & 0 & A^T P & \bar{\bar{C}}^T & {G_1}^T \varepsilon \\ * & * & -\gamma^2 I & \bar{B}^T P & \bar{\bar{D}}^T & {G_2}^T \varepsilon \\ * & * & * & -P & 0 & 0 \\ * & * & * & * & -I & * \\ * & * & * & * & * & -\varepsilon I \end{bmatrix} < 0 \tag{34}$$

Using Theorem 1, seeking a minimum value of γ satisfies the following Equation 35

$$\|G_{B_a}\|_\infty < \gamma \Leftrightarrow \|G_1(zI - A - \Delta A)^{-1}(B + \Delta B \quad E_d) + (G_2 \quad 0)\|_\infty < \gamma \tag{35}$$

Hence, Equation 32 becomes Equation 36:

$$J_{th} = \|G_{r\overline{ud}}\|_\infty (\delta_{\Delta s})\,[\,\gamma.(\delta_{dd} + \|u(z)\|_2)] + \delta_{dd} \tag{36}$$

To this end, the only unknown is $\|G_{r\overline{ud}}\|_\infty$ to compute the proposed threshold. The following lemma provides the solution of$\|G_{r\overline{ud}}\|_\infty$.

Lemma 2 (Ding, 2013): Given an LTI system, $G_{r\overline{ud}}(z) = C(zI - A + LC)^{-1}\bar{E}_{\bar{\bar{u}}} + \bar{F}_{\bar{\bar{u}}}$, and for given $\bar{\gamma}_d > 0$ if there exists a symmetric matrix P such that the following LMI Equation 37 holds then $\|G_{r\overline{ud}}(z)\|_\infty < \bar{\gamma}_d$

$$\begin{bmatrix} -P & P(A - LC) & P\bar{E}_{\bar{\bar{u}}} & 0 \\ * & -P & 0 & C^T \\ * & * & -\bar{\gamma}_d I & {\bar{F}_{\bar{\bar{u}}}}^T \\ * & * & * & -\bar{\gamma}_d I \end{bmatrix} < 0, \quad P > 0 \tag{37}$$

Solving LMI Equation 37 in MATLAB and minimum $\bar{\gamma}_d$ can be found at which a feasible solution of LMI Equation 37 is obtained. Finally, we are able to write the final expression of the adaptive threshold in Equation 36 as Equation 38:

$$J_{th} = \bar{\gamma}_d.(\delta_{\Delta s}\,\gamma\,(\delta_{dd} + \|u(z)\|_2) + \delta_{dd}) \tag{38}$$

Rearranging Equation 37 gives Equation 39:

$$J_{th} = \bar{\gamma}_d \delta_{\Delta s}\,\gamma\,\delta_{dd} + \bar{\gamma}_d \delta_{\Delta s}\,\gamma\,\|u(z)\|_2 + \bar{\gamma}_d \delta_{dd} \tag{39}$$

Denoting, $\gamma_u = \bar{\gamma}_d \delta_{\Delta s}\gamma$ and $\gamma_d = \bar{\gamma}_d(1 + \delta_{\Delta s}\gamma)$

By correlating Equations 13 and 39, unknown adaptive threshold parameters can be obtained. It is worth remembering that robust threshold design Equation 39 depends on the system parameters and control input. Furthermore, FD is independent of the residual generator design. A fault can be successfully detected when an evaluated residual using Equation 6 crosses the threshold of Equation 39.

Algorithm for Computation of Adaptive Threshold

Step 1: Define the matrices according to Equations 16 and 24

Step 2: Find the minimum value of γ using Theorem 1 for the given value of δ_{dd} and $\delta_{\Delta s}$

Step 3: Find the minimum value of $\bar{\gamma}_d$ using Lemma 2

Step 4: Compute the residual evaluation function using Equation 6

Step 5: Calculate the online value of $\|u(k)\|_2$

Step 6: Set J_{th} according to Equation 38

Step 7: Compare the evaluated residual, $J(k)$, in Equation 6 with the threshold, J_{th}, in Equation 38 such that $J(k) \leq J_{th}$ is fault-free and vice versa.

SIMULATION RESULTS

The performance of the FD system based on the proposed threshold is examined through simulations. Two system models are tested: (1) A DC motor system and (2) A three-tank benchmark system. For simulation purposes, two types of faults are considered: (1) Abrupt fault and (2) Intermittent fault. Since the system's behavior changes dramatically and could potentially harm its stability, abrupt faults seem severe for the system. The sensors and actuators of the system also frequently experience intermittent faults that degrade the system's performance. These faults are introduced to show how well the proposed method can identify critical faults.

Application to a DC Motor System

A linear discrete-time model of a DC motor with nominal system matrices is shown below:

$$A = \begin{bmatrix} 0.2592 & 0.0017 \\ -0.0033 & 0.0025 \end{bmatrix}, \quad E_f = B = \begin{bmatrix} 0.0148 \\ 0.9974 \end{bmatrix}$$

$$E_d = \begin{bmatrix} -1.6460 \\ 0.0148 \end{bmatrix}, \quad C = [1 \quad 0], \quad F_d = F_f = 1$$

ω_m and i_a are the state variables, defined as angular velocity and armature current of the DC motor, respectively. Model uncertainty is represented as:

$$H_1 = \text{diag}[0.1 \quad 0.1], H_2 = [0.1 \quad 0]$$

$$G_1 = \text{diag}[0.1 \quad 0.1], G_2 = [0 \quad 0.1]^T$$

For simulations, the unknown parameter ($\Sigma = \text{diag}[0.9597, 0.9597]$) of the norm-bounded model, uncertainty, is chosen randomly. Load torque variation is treated as an unknown input to the DC motor that holds the bounded condition, i.e., $d(k) \in [-0.01, 0.01]$. Furthermore, matrix $A + \Delta A$ is stable if ΔA holds the condition in Equation 2. Sensor fault is considered in this simulation that occurs in the speed sensor of the DC motor.

Control input $u(k)$ (Figure 1) is applied to the DC motor for simulation. As stated previously, the algorithm to find the unknown parameters of the adaptive threshold is implemented in MATLAB.

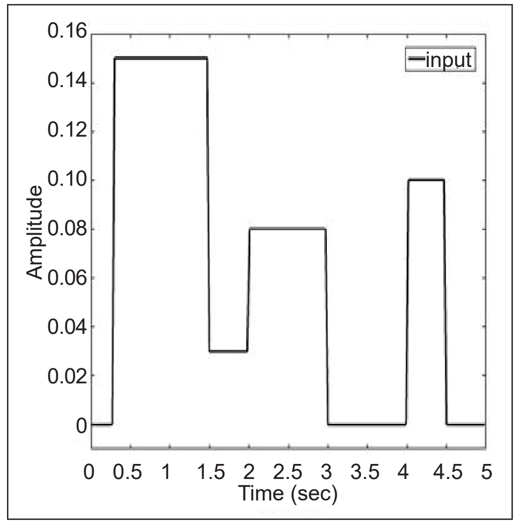

Figure 1. Control input to DC motor

By referring to Equation 38, i.e., $J_{th} = \gamma_u \|u(k)\|_2 + \gamma_d \delta_{dd}$ where $\gamma_u = \bar{\gamma}_d \delta_{\Delta s} \gamma$ and $\gamma_d = \bar{\gamma}_d (1 + \delta_{\Delta s} \gamma)$, $\delta_{dd} = 0.005$ and $\delta_{\Delta s} = 0.5155$ is taken for threshold computation. $\|u(k)\|_2$ is the l_2 l_2 norm of the control input, known during the system's operation. The only unknown parameters in J_{th} are γ and $\bar{\gamma}_d$, which can be determined easily by solving Equations 34 and 36 using the MATLAB LMI toolbox. After several iterations, γ and $\bar{\gamma}_d$ are reduced to 0.4029 and 1.9135, respectively. For a residual generation, observer structure Equation 3 is used, and filter gain *L*, using Lemma 2, is calculated as:

$$L = \begin{bmatrix} -0.2592 \\ 0.0016 \end{bmatrix}$$

Figure 2 represents the abrupt speed sensor fault detection using the proposed and standard thresholds. At *t* = 2 seconds, the speed sensor experiences an abrupt fault. An abrupt fault of extremely small magnitude is simulated as a step function of 0.1 amplitude. It can be observed that the evaluation function is below the detection threshold in the case of a fault-free sensor with a certain amount of false alarms, but the residual evaluation function crosses the adaptive threshold at the time of fault occurrence, which shows the explicit demonstration of the FD in the sensor. The evaluated residual is also compared with the state-of-the-art threshold Equation 7, stated in the literature for the same type of speed sensor fault. It is evident from Figure 2 that if a threshold using Equation 7 is selected, there are missed detections of the faults. Missed detection of the faults causes the FD system's performance to decrease, ultimately leading to monitored system failure. The effectiveness of the proposed threshold can be observed in Figure 2. It becomes obvious that the effect of a fault is considerably increased using the proposed threshold Equation 38 with negligible false alarms, which delivers fast detection of the fault. Faults cannot be detected accurately using a standard threshold, irrespective of zero false alarms.

In Figure 3, an intermittent sensor fault, which shows the improper functioning of the sensor, is simulated for FD. Figure 3 demonstrates that the evaluated residual is above the threshold for the time of fault occurrence. Both types of sensor faults are successfully detected using the adaptive threshold technique. Thus, these findings support the efficacy

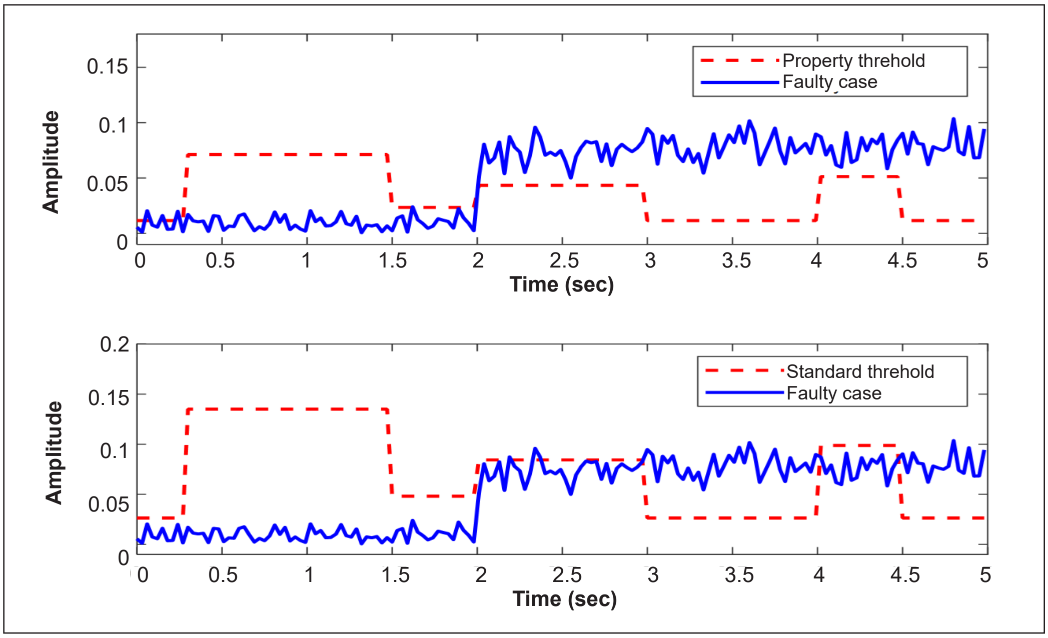

Figure 2. Abrupt sensor FD: proposed threshold (top), standard threshold (bottom)

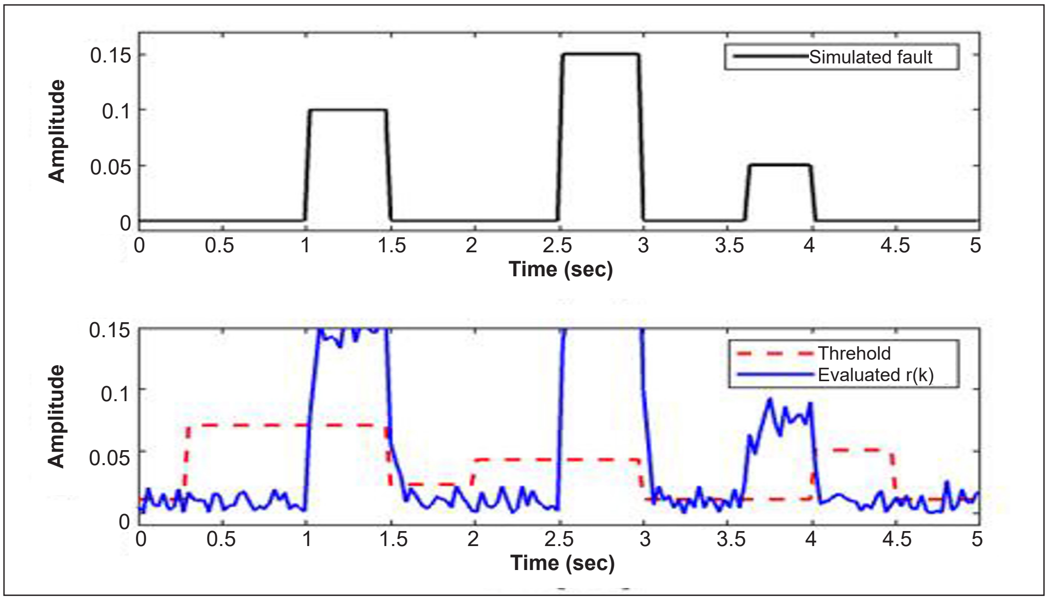

Figure 3. Simulated intermittent sensor fault (top) and fault detection (bottom)

of the proposed approach by accurately and quickly identifying the sensor fault in the DC motor regardless of unknown disturbances and model uncertainty in the system state matrix as well as in the input and measurement matrices.

Application to a Three-tank System

As seen in Figure 4, the three-tank system is a benchmark system that has been extensively studied in chemical engineering. It is employed in real-time software and practical applications to implement various control and FD techniques. The three-tank system's dynamics are nonlinear. Linearizing the nonlinear model introduces modeling errors that are considered norm-bound model uncertainty. It makes it a useful benchmark for FD algorithm testing.

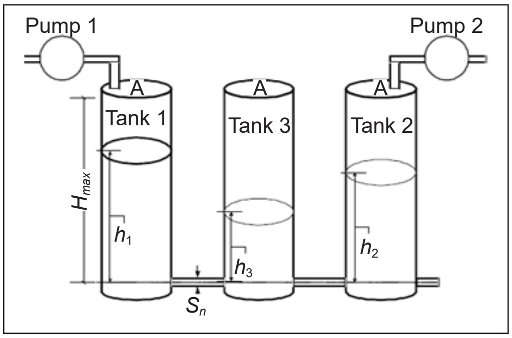

Figure 4. Three-tank system (Ding, 2013)

The following equations express the nonlinear dynamics of the three-tank system and are represented in Equation 40:

$$\begin{aligned} A\dot{h}_1 &= Q_1 - Q_{13} \\ A\dot{h}_2 &= Q_2 + Q_{32} - Q_{20} \\ A\dot{h}_3 &= Q_{13} - Q_{32} \end{aligned} \tag{40}$$

with

$$Q_{13} = a_1 s_{13} sgn(h_1 - h_3)\sqrt{2g|h_1 - h_3|}$$

$$Q_{32} = a_3 s_{23} sgn(h_3 - h_2)\sqrt{2g|h_3 - h_2|}$$

$$Q_{20} = a_2 s_0 \sqrt{2gh_2}$$

Water levels h_1, h_2 and h_3 in respective tanks are the process outputs $y(k)$, while mass flows Q_1, Q_2 are taken as the process inputs $u_1(k)$, $u_2(k)$. The mass flow from the ith tank to the jth tank is represented by Q_{ij}. The cross-sectional areas of the pipe linking tank 1-tank 3 and tank 2-tank 3 are represented by S_{13} and S_{23}, respectively. S_0 is the cross-sectional area of the tank 2 outlet pipe. The signum function, abbreviated as sgn, is described as:

$$\text{sgn}(x) = \begin{cases} -1 & if x < 0 \\ 0 & if x = 0 \\ 1 & if x > 0 \end{cases}$$

$$s_{13} = s_{23} = s_0 = s_n$$

Table 1 lists the system's coefficients and relevant parameters. The disturbance in the three-tank system is caused by the water bubbles produced as a result of the pumps' water released into the tanks. There is also measurement noise in the sensors that determines the water levels. The system's linear model is developed for FD by expanding Taylor's series around the equilibrium or operating point using the linearization approach. A discrete-time linear model, expressed in the state-space form (1), is obtained by performing the linearization at the operating points $h_1 = 45$ cm, $h_2 = 15$ cm h_3 and = 30 cm, and discretizing the linearized model at a sampling time of 1 second. Nominal matrices are defined as:

$$A = \begin{bmatrix} 0.9915 & 0 & 0.0084 \\ 0 & 0.9807 & 0.0082 \\ 0.0084 & 0.0082 & 0.9833 \end{bmatrix}, C = \text{diag}[1,1,1]$$

$$B = \begin{bmatrix} 0.0065 & 0.0008 \\ 0.0008 & 0.0065 \\ 0 & 0 \end{bmatrix}, E_d = \begin{bmatrix} 0.25 & 0 & 0 \\ 0 & 0.25 & 0 \\ 0 & 0 & 0.25 \end{bmatrix}$$

$$D = 0, E_f = B, F_d = F_f = C$$

The modeling errors brought in by the linearization process, defined below, represent the model uncertainty in the system matrices.

$$H_1 = H_2 = \begin{bmatrix} -0.01 & 0 & 0 \\ 0 & -0.01 & 0 \\ 0 & 0 & -0.01 \end{bmatrix}$$

$$G_1 = \begin{bmatrix} 0.01 & 0 & 0.015 \\ 0 & 0.01 & 0.015 \\ 0.01 & 0.01 & 0.05 \end{bmatrix}$$

The same procedure simulates the model, with a constant inflow of pumps $Q_1 = 100$ cm^3/sec, $Q_2 = 100$ cm^3/sec, uniform disturbance, $d(k) \in [-0.01, 0.01]$. l_2 norm of the

Table 1
Parameters of the three-tank system

Parameters	Symbol	Value	Unit
Cross-section area of the tank	A	154	cm^2
Cross-section area of the pipe	S_n	0.5	cm^2
Maximum height of the tank	H_{max}	62	cm
Maximum flow rate of pump 1	$Q1_{max}$	100	cm^3/sec
Maximum flow rate of pump 2	$Q2_{max}$	100	cm^3/sec
Coefficient of flow for pipe 1	a_2	0.46	
Coefficient of flow of pipe 2	a_2	0.60	
Coefficient of flow for pipe 3	a_3	0.45	

control input is determined online. $\delta_{dd} = 0.005$ and $\delta_{\Delta s} = 0.5155$ are the energy levels of disturbance and model uncertainty, respectively. MATLAB LMI toolbox is used to compute the unknown parameters, γ and $\bar{\gamma}_d$, in J_{th} by solving Equations 34 and 36, respectively. After several iterations, γ and $\bar{\gamma}_d$ are reduced to 0.023 and 1.006, respectively.

For a residual generation, observer gain L is calculated using Lemma 2 as:

$$L = \begin{bmatrix} 0.2461 & 0 & 0 \\ * & 0.2461 & 0 \\ * & * & 0.2461 \end{bmatrix}$$

One of the three sensors' offset faults is taken into account during the simulation. The offset value ranges from 0 to H_{max} . In this regard, at $t = 80$ seconds, a 2 cm offset sensor fault is introduced into the sensor of tank 3.

It can be shown from Figure 5 that fault detectability using the proposed threshold is significantly improved as compared to a standard threshold. However, there are false alarms in the system that are in an acceptable range and do not affect the FD system's performance. Similar results are obtained for the sensor intermittent fault in tank 1 and abrupt actuator fault in pump 1 in Figures 6 and 7, respectively. It can be noticed from the simulation results of both benchmark systems that fault detection is quite easier using the proposed threshold. The reason is the improved fault detectability of the proposed threshold.

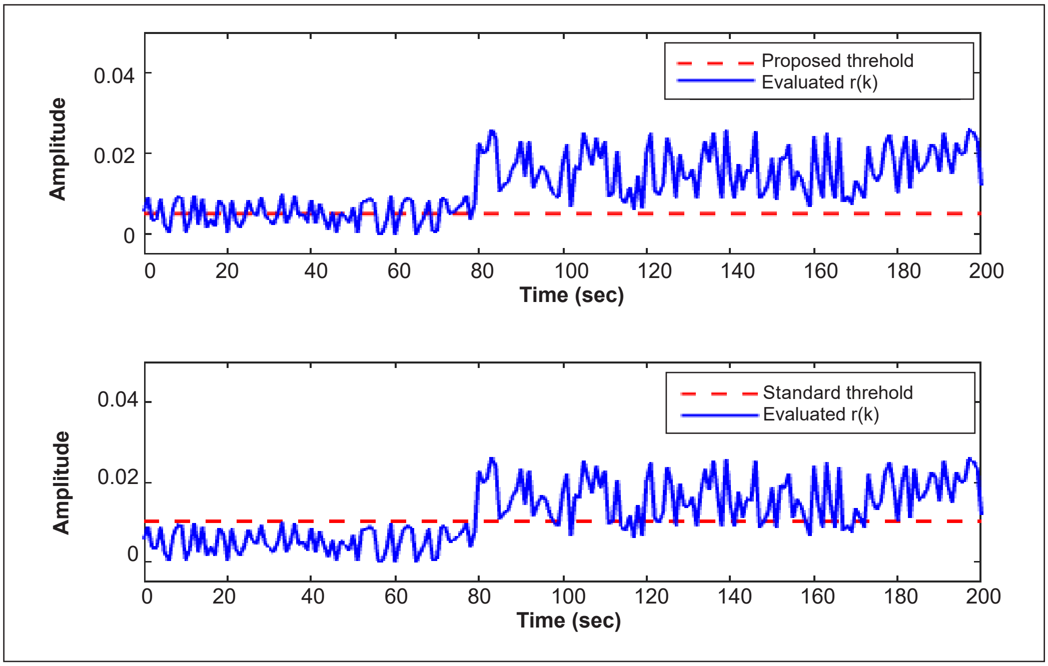

Figure 5. Abrupt sensor FD in tank 3: proposed threshold (top), standard threshold (bottom)

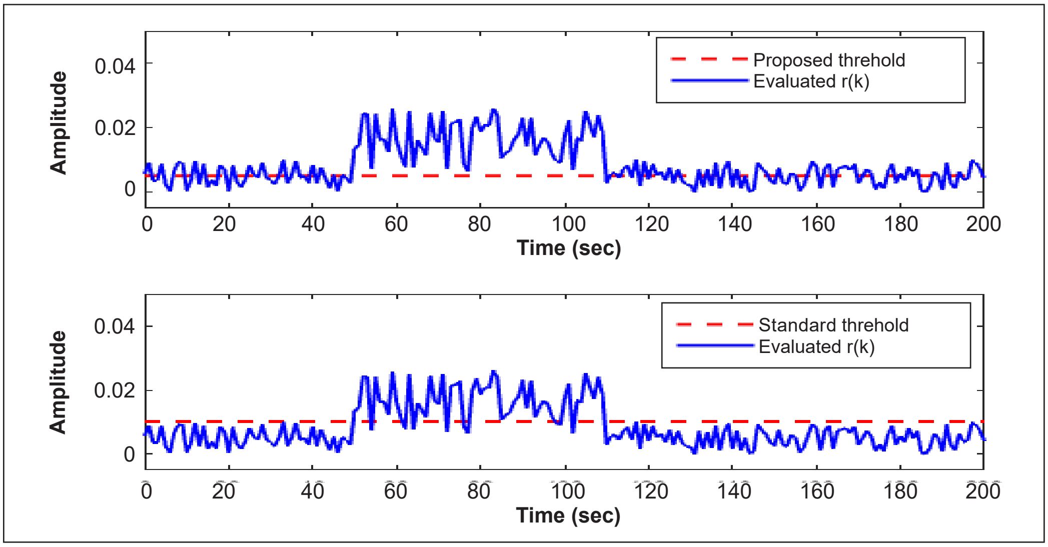

Figure 6. Intermittent sensor FD in tank 1: proposed threshold (top), standard threshold (bottom)

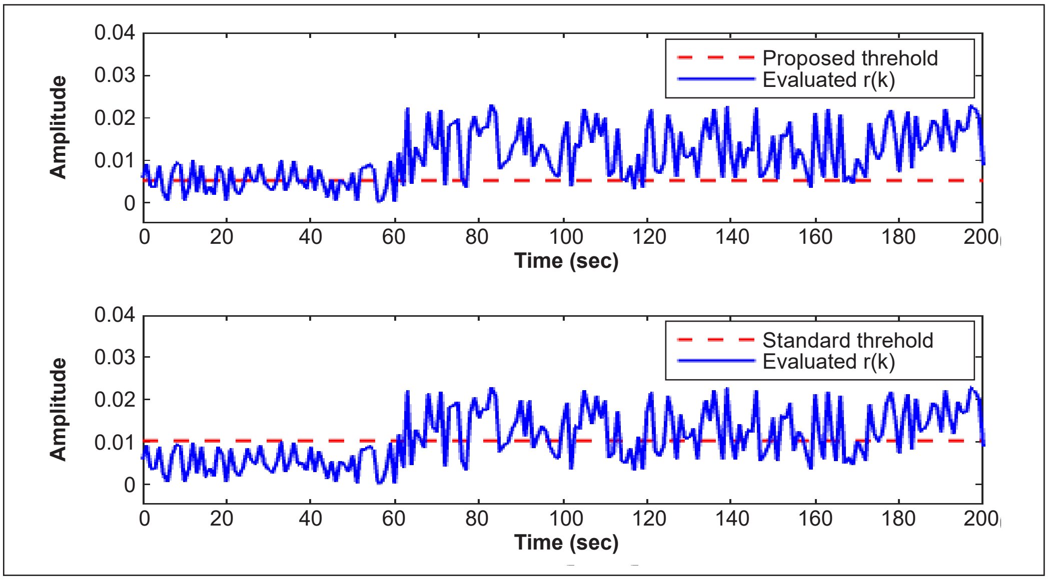

Figure 7. Abrupt actuator FD in pump 1: proposed threshold (top), standard threshold (bottom)

CONCLUSION

An adaptive threshold-based fault detection system has been designed for linear systems subjected to norm-bounded model uncertainty and a deterministic disturbance signal. The computation of unknown threshold parameters is formulated as an H_∞ optimization. The main contribution of this paper is the design of an adaptive threshold and its integration into a fault detection system, such that fault detectability is improved. Due to the integrated design, a separate design for the robust residual generator is not required. It is shown that the proposed threshold is a linear function of unknown disturbances and known control inputs that are available for online computation. The performance of the proposed approach is verified by simulations of two well-known applications for different kinds of faults. Results show that all faults were successfully detected.

ACKNOWLEDGMENTS

The work is supported by the Ministry of Higher Education Malaysia for Fundamental Research Grant Scheme with Project Code: FRGS/1/2019/TK04/USM/02/12 and the HRDI-UESTPS scholarship program funded by the Higher Education Commission (HEC) of Pakistan.

REFERENCES

Ahmad, M., & Mohd-Mokhtar, R. (2021). Fault detection full order filter apply to discrete time-invariant linear system. *Journal of Engineering Science and Technology, 16*(5), 4221-4234.

Ahmad, M., & Mohd-Mokhtar, R. (2022). A survey on model based fault detection techniques for linear time invariant systems with numerical analysis. *Pertanika Journal of Science & Technology, 30*(1), 53-78. https://doi.org/10.47836/pjst.30.1.04

Ammiche, M., Kouadri, A., Halabi, L. M., Guichi, A., & Mekhilef, S. (2018). Fault detection in a grid-connected photovoltaic system using adaptive thresholding method. *Solar Energy, 174*, 762-769. https://doi.org/10.1016/j.solener.2018.09.024

Blanke, M., Kinnaert, M., Lunze, J., & Staroswiecki, M. (2015). *Diagnosis and Fault-Tolerant Control* (3rd ed.). Springer.

Boyd, S., El Ghaoui, L., Feron, E., & Balakrishnan, V. (1994). *Linear Matrix Inequalities in System and Control Theory*. Society for Industrial and Applied Mathematics.

Chen, J., & Patton, R. J. (2012). *Robust Model-Based Fault Diagnosis for Dynamic Systems*. Springer Science & Business Media.

Ding, S. X. (2013). *Model-Based Fault Diagnosis Techniques: Design Schemes, Algorithms, and Tools*. Springer Science & Business Media.

Ding, S. X. (2014). *Data-Driven Design of Fault Diagnosis and Fault-Tolerant Control Systems*. Springer Science & Business Media.

Gertler, J. J. (2017). *Fault Detection and Diagnosis in Engineering Systems*. CRC Press.

Isermann, R. (2006). *Fault Diagnosis Systems*. Springer.

Montes de Oca, S., Puig, V., & Blesa, J. (2012). Robust fault detection based on adaptive threshold generation using interval LPV observers. *International Journal of Adaptive Control and Signal Processing, 26*(3), 258-283. https://doi.org/10.1002/acs.1263

Na, Y., & Ahmad, M. (2019). A fault detection scheme for switched systems with noise under asynchronous switching. In *9th International Conference on Information Science and Technology* (pp. 258-262). IEEE Publishing. https://doi.org/10.1109/ICIST.2019.8836838

Rahnavard, M., Ayati, M., Yazdi, M. R. H., & Mousavi, M. (2019). Finite time estimation of actuator faults, states, and aerodynamic load of a realistic wind turbine. *Renewable Energy, 130*, 256-267. https://doi.org/10.1016/j.renene.2018.06.053

Puig, V., Montes de Oca, S., & Blesa, J. (2013). Adaptive threshold generation in robust fault detection using interval models: Time-domain and frequency-domain approaches. *International Journal of Adaptive Control and Signal Processing, 27*(10), 873-901. https://doi.org/10.1002/acs.2362

Raka, S. A., & Combastel, C. (2013). Fault detection based on robust adaptive thresholds: A dynamic interval approach. *Annual Reviews in Control, 37*(1), 119-128. https://doi.org/10.1016/j.arcontrol.2013.04.001

Salimi, A., Batmani, Y., & Bevrani, H. (2019). Model-based fault detection in DC microgrids. In *2019 Smart Grid Conference* (SGC) (pp. 1-6). IEEE Publishing. https://doi.org/10.1109/SGC49328.2019.9056589